Biomaterials 33 (2012) 6495–6506

Contents lists available at SciVerse ScienceDirect

Biomaterials

journal homepage: www.elsevier.com/locate/biomaterials

Overcoming multidrug resistance by co-delivery of Mdr-1 and survivin-targeting RNA with reduction-responsible cationic poly(β-amino esters)

Qi Yin, Jianan Shen, Lingli Chen, Zhiwen Zhang, Wangwen Gu, Yaping Li*

Center of Pharmaceutics, Shanghai Institute of Materia Medica, Chinese Academy of Sciences, 501, Haike Road, Shanghai 201203, China

ARTICLE INFO

Article history:
Received 11 April 2012
Accepted 17 May 2012
Available online 15 June 2012

Keywords:
Poly(β-amino esters)
RNA
P-glycoprotein
Survivin
Multidrug resistance

ABSTRACT

Multidrug resistance (MDR) remains one of the main challenges in the successful chemotherapy of human cancer. RNA interference (RNAi) strategy aiming at only one cause of MDR was widely applied, nevertheless hardly obtained satisfactory tumor-suppressing effect. In this work, a new attempt to package two kinds of RNA with different functions into one vector and reverse MDR against two different mechanisms via RNAi was carried out. A new bioreducible poly (β-amino esters) (PAEs), poly[bis(2-hydroxylethyl)-disulfide-diacrylate-β-tetraethylenepentamine] (PAP) was synthesized by Michael addition reaction. The PAEs/RNA complex nanoparticles (PAEN) were prepared. The experimental results demonstrated that co-delivery of iMdr-1-shRNA and iSurvivin-shRNA could be achieved by a single vector, and interfering two genes simultaneously had a synergistic effect on overcoming MDR. PAEN lowered the IC_{50} value of doxorubicin (DOX) in MDR tumor cells to a comparable level to that in the sensitive cell line through down-regulating the expression of P-gp and Survivin, and decreased the tumor volumes in mice xenograft model bearing DOX-resistant human breast cancer when combined with DOX. These results illustrated that PAEN could be applied as potential efficient non-viral RNA carriers for reversing MDR.

1. Introduction

Multidrug resistance (MDR) remains one of the main challenges in the successful chemotherapy of human cancer [1]. The mechanism of MDR is very complicated, but the over-expression of ATP-binding cassette (ABC) transporters, which are trans-membrane proteins functioning as pumps that extrude toxins and drugs out of the cells, and the blocked apoptosis pathway, are two main causes of MDR [2,3]. P-glycoprotein (P-gp), one of the most well-described ABC transporters, is over-expressed in the malignant tissues of almost 40–50% of breast cancer patients and becomes an attractive target to overcome MDR [4]. Survivin, a new member of the inhibitors of apoptosis (IAP) family, has functional role in both cell division and apoptosis control, and is often found to be up-regulated in cancers, enabling it a potential new target for cancer treatment [5].

In order to overcome MDR, some small-molecule compounds were used as functional inhibitors, such as verapamil [6], cyclosporine A [7] and promethazine [8], but their unpredicted pharmacokinetic interaction with chemotherapeutics and toxicities limited their usage in clinics [9]. Also, it was reported that the chemotherapeutic agents encapsulated into nanoparticles could evade the drug efflux pumps and increase the intracellular drug concentration, whose *in vivo* anti-tumor effects were rarely shown [10–12]. Additionally, such an increase in the concentration did not result in a proportionate increase in cell death when the apoptosis pathway was blocked. Recently, it was reported that MDR could partly be reversed by silencing the expression of the gene encoding P-gp, i.e., Mdr-1 or Survivin via RNA interference (RNAi) with only a single gene knocked down at one time [13–18], but the IC_{50} values of chemotherapeutics agent in MDR cancer cells were still notably higher than that in sensitive cell lines, and their *in vivo* anti-tumor experiments only exhibited the capability to slow down the tumor growth but not to decrease the tumor volume. Additionally, an efficient carrier is required to deliver therapeutic small interference RNA (siRNA) or short hairpin RNA (shRNA) to the target site because there are many natural barriers to overcome [19].

Poly (β-amino esters) (PAEs) is a kind of biodegradable polymer containing amino segments and acid or base-sensitive ester bonds, which makes PAEs be able to condense nucleic acid molecules at physiological pH and release them into cytoplasm at acidic endosomal or lysosomal environment [20]. Although there have been reports about employing PAEs as RNA vehicles [21–23], the RNAi efficiency was not as high as expected, which could be because the degradation of PAEs in the weak acidic intracellular environment was not rapid enough for timely release of RNA.

* Corresponding author. Tel./fax: +86 21 2023 1979.
E-mail address: ypli@mail.shcnc.ac.cn (Y. Li).

0142-9612/$ – see front matter © 2012 Elsevier Ltd. All rights reserved.
doi:10.1016/j.biomaterials.2012.05.039

In this work, we designed an approach to reverse MDR by co-delivery of Mdr-1 and Survivin-targeting RNA with reduction-responsible cationic PAEs, which was introduced reduction-sensitive disulfide bonds into the framework. The disulfide bond tends to be cleaved under the high concentration of reductive glutathione and thioredoxin reductase in the intracelluar circumstance and triggers the degradation of the disulfide linkage-containing polymers. At first, a new PAE, poly[bis(2-hydroxylethyl)-disulfide-diacrylate-β-tetraethylenepentamine] (PAP) was synthesized by Michael addition reaction. Then, the PAEs/RNA complex nanoparticles were prepared, and their effects on P-gp expression, Survivin expression, DOX uptake, DOX IC_{50} value, cell apoptosis and cell cycle of MDR tumor cells were evaluated. Finally, their anti-tumor abilities on mice xenograft model bearing MDR cancer were also investigated. This approach was a new attempt to package two kinds of RNA with different functions into one vector and reverse MDR against two different mechanisms via RNAi. It was expected that the combination of PAEs-based RNAi and chemotherapy could overcome MDR in tumor and there would be synergistic effect by interfering two different genes.

2. Materials and methods

2.1. Materials

Bis(2-hydroxylethyl) disulfide, acryloyl chloride were purchased from Alfa Aesar (Tianjin, China). Trypsin-EDTA and agarose were obtained from Gibco-BRL (Burlington, ON, Canada). The RPMI 1640 medium, YOYO-1 and sodium azid were purchased from Invitrogen GmbH (Karlsruhe, Germany). Fetal bovine serum (FBS) was purchased from Biochrom AG (Berlin, Germany). Ethidium bromide (EB), 3-(4,5-dimethylthiazol-2-yl)-2,5-diphenyltetrazolium bromide (MTT), sodium ascorbate, trypan blue and branched polyethylenimine (PEI, 25 kDa) were purchased from Sigma (St. Louis, MO). Phyeoerythin (PE)-labled anti-human P-glycoprotein (CD243) or PE-labled mouse IG2a isotype control were purchased from eBioscience (CA, USA). Fix & Perm® cell permeabilization reagents were purchased from Multi-Sciences Biotech (Shanghai, China). Carboxyfluorescein (CFS)-conjugated anti-human Survivin and CFS-conjugated mouse IgG_1 isotype control were purchased from R & D Systems Inc. (Shanghai, China). Other chemicals if not mentioned were obtained from Sinopharm Group Chemical Reagent Co., Ltd. and of analytical grade.

The PGPHI/GFP/Neo-NM_000927-expressing pDNA (iMdr-1-shRNA) that targets the sequence AATGTTGTCTGGACAAGCACT, pGPU6/Neo-SurvivinshRNA-expressing pDNA (iSurvivin-shRNA) that targets the sequence GAATTAACCCTTGGTGAAT and pGPU6/Neo-negative control shRNA-expressing pDNA (NC-shRNA) that targets the sequence GTTCTCCGAACGTGTCACGT were obtained from GenePharm Co. Ltd. (Shanghai, China) and purified with the Plasmid Maxi Kit (Qiagen GmbH, Hilden, Germany) in accordance with the manufacturer's instructions. The purity was confirmed by UV spectrophotometry (A260/A280) and the concentration was determined from the absorbance at 260 nm.

2.2. Cell culture

The cell lines MCF7 (human breast adenocarcinoma cell line) cells were obtained from the American Type Culture Collection (ATCC, Manassas, VA). The MCF7 cells resistant to doxorubicin (MCF7/ADR cells) were purchased from Keygen Biotech. Co., Ltd. (Nanjing, China). MCF7 cells were cultured in RPMI 1640 medium containing 10% FBS, 100 Unit/mL penicillin G sodium and 100 μg/mL streptomycin sulfate (complete 1640 medium). MCF7/ADR cells were grown in complete 1640 medium with 1 μg/mL doxorubicin (DOX). Cells were maintained at 37 °C in a humidified and 5% CO_2 incubator.

2.3. Animals

Male BALB/c nude mice aged 6 weeks (18–22 g) were purchased from Shanghai experimental animal center (Shanghai) and kept under a 12 h light/dark cycle at the Animal Care Facility. The animals were given daily fresh diet with free access to water and acclimatized for at least 5 days prior to the experiments. The *in vivo* experiments were carried out under the guideline approved by the Institutional Animal Care and Use Committee of the Shanghai Institute of Materia Medica, Chinese Academy of Sciences.

2.4. Synthesis of poly[bis(2-hydroxylethyl)-disulfide-diacrylate-β-tetraethylenepentamine]

Disfulfide-based diacrylate (DSA) and poly[bis(2-hydroxylethyl)-disulfide-diacrylate-β-triethylenetetramine] (PAT) were synthesized as described in our previous work [24]. Synthesis of poly[bis(2-hydroxylethyl)-disulfide-diacrylate-β-tetraethylenepentamine] (PAP) was carried out by Michael addition reaction between Tetraethylenepentamine (TEPA) and DSA (Fig. 1A). Briefly, 0.5 g (1.9 mmol) of DSA dissolved in 2 mL of anhydrous DCM was added into a solution of 0.54 g (2.85 mmol) of TEPA in 2 mL of anhydrous DCM. The reaction was performed at 45 °C in the dark under nitrogen for 5 days. The resulted solution was precipitated into 50 mL of hexane under vigorous stirring. The polymer was dried under vacuum for 1 day at room temperature and dialyzed against deionized water for 72 h. Water was removed by rotation evaporation, and the polymer was dried under vacuum overnight. The yield of the polymer was 43%.

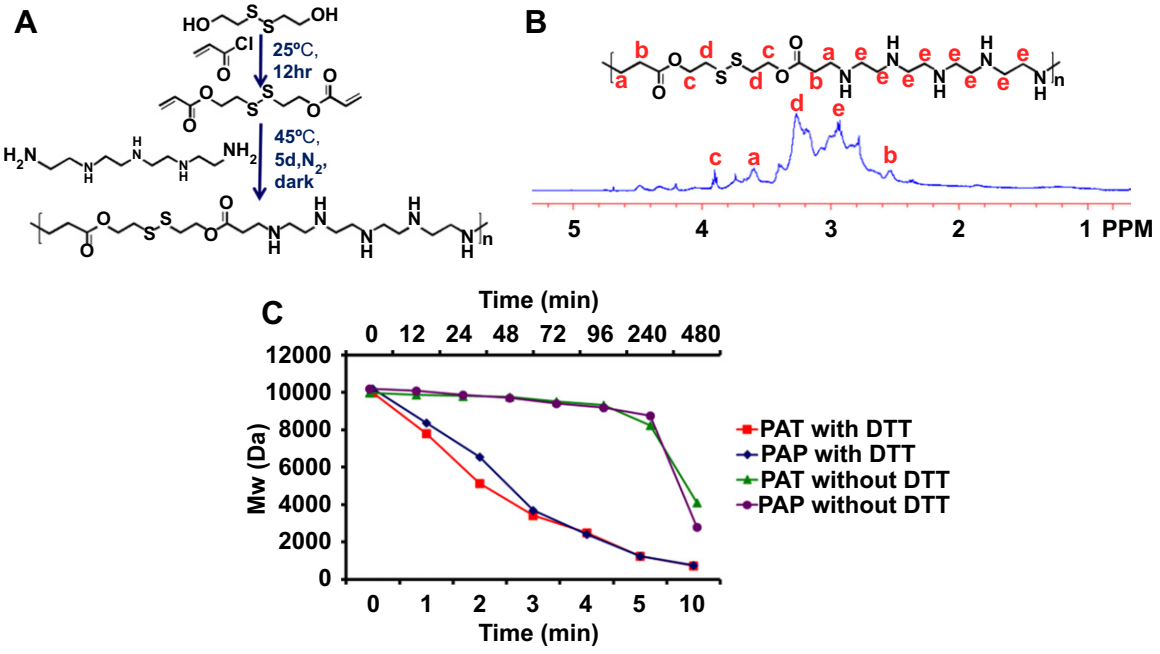

Fig. 1. Synthesis and characterization of PAE. (A) Scheme for synthesis of PAP; (B) ^1H NMR spectra of PAP; (C) Degradation curves of PAT and PAP (The upper *x*-axis: incubated without DTT, the lower *x*-axis: incubated with DTT).

The structure of polymer was confirmed by ^{1}H NMR spectra recorded on Varian Mercury Plus-400 NMR spectrometer (Varian, USA) operating at 400 MHz. The molecular weight (Mw) and polydispersity (Mw/Mn) of PAP were measured by a gel permeation chromatography (GPC) system relative to dextran standards (Mp = 4400–401000 Da, American Polymer Standards Corporation, USA). GPC was performed on a Waters 2695 controller equipped with Ultrahydrogel columns (250 PKGD and 1000 PKGD, 30 °C) and a refractive index detector (model 2414). 0.05% NaN_3 aqueous solution was used as mobile phase with a flow rate of 0.5 mL/min.

To investigate the hydrolytic degradation of PAEs (PAP and PAT), 10 mg of PAEs were dissolved in 2 mL PBS (pH 7.4) and incubated at 37 °C. 150 μL of the solution was taken every 24 h and analyzed by GPC. To estimate the reductive degradation, 0.35 mg DTT and 10 mg of PAEs were dissolved in 2 mL PBS (pH 7.4) and incubated at 37 °C. 150 μL of the solution was taken every 5 min and analyzed by GPC.

2.5. Preparation and characterization of PAEs/RNA complex nanoparticles

PAP/RNA complex nanoparticles (PAPN) were prepared as following: briefly, shRNA solution was added into the PAE solution while vortexing to make a solution with shRNA final concentration of 0.125 μg/μL and various polymer nitrogen to RNA phosphate (N/P) ratios. Then the solution was vortexed for 30 s and incubated at room temperature for 30 min. Complex formation was confirmed by agarose gel retardation on 1.0% agarose gel in Tris-Acetate-EDTA (TAE) buffer containing 0.5 μg/mL EB for 45 min at 80 V. The resulting shRNA migration pattern was visualized with a UV illuminator. The particle size and zeta potential of PAEN were measured by the laser light scattering measurement using a Nicomp 380/ZLS zeta potential analyzer (Particle Sizing System, USA). PAT/RNA complex nanoparticles (PATN) were also prepared by the same procedure as described above.

2.6. Cytotoxicity of PAEN

The cytotoxicity of PAEN was determined by MTT assay. MCF7 and MCF7/ADR cells were seeded in 96-well plates at a density of 6×10^3 cells per well. After 24 h incubation, the media was replaced with antibiotic-free RPMI-1640 containing PAEN at various concentrations. After culturing for 48 h, MTT was added to each well at a final concentration of 0.5 mg/mL, followed by 4 h incubation. Then the supernatant was removed, and the resulting formazan was dissolved in 200 μL DMSO. The absorbance at 570 nm was read on microplate reader (Tecan Infinite F200, Salzburg, Austria). Viability of the non-treated cells was defined as 100%.

2.7. In vitro shRNA expression

MCF7/ADR cells were seeded in 24-well plates at a density of 5×10^4 cells per well in 500 μL RPMI 1640 medium. After attachment, cells were incubated with PAT/iMdr-1-shRNA complex nanoparticles (PATmN), PAP/iMdr-1-shRNA complex nanoparticles (PAPmN) or branched PEI 25K/iMdr-1-shRNA complex nanoparticles (PEImN) with various N/P ratios for 24 h. Then the medium was changed to fresh RPMI 1640 medium, and the cells were incubated at 37 °C for another 24 h. The shRNA expression efficiency was determined through the expression of the co-expressed EGFP by visualization under a fluorescence microsope (Olympus, Japan) and the measurement of fluorescent intensity on a FACSCalibur system (Becton Dickinson, USA). The optimal N/P ratios of each kind of nanoparticles for RNAi were chosen according to the shRNA expression experiment.

2.8. Gene silencing experiment

MCF7 and MCF7/ADR cells were seeded in 24-well plates at a density of 5×10^4 cells per well and incubated overnight followed by addition of PATmN, PAPmN, PEImN, PAT/iSurvivin-shRNA complex nanoparticles (PATsN), PAP/iSurvivin-shRNA complex nanoparticles (PAPsN), PAT/NC-shRNA complex nanoparticles (PATnN), PAP/NC-shRNA complex nanoparticles (PAPnN), branched PEI 25K/iSurvivin-shRNA complex nanoparticles (PEIsN) or branched PEI 25K/NC-shRNA complex nanoparticles (PEInN) at optimal N/P ratios to reach a final concentration of 2.5 μg RNA in 500 μL media per well. After 24 h incubation, the media were replaced with fresh media and incubated for 24 h.

For P-gp expression study, cells were trypsinized and washed twice with PBS (pH 7.4). Then the cells were resuspended in 100 μL PBS, and PE-labled anti-human P-glycoprotein (CD243) or PE-labled mouse IG2a isotype control was added and followed by 30 min incubation. After 400 μL PBS was added, and centrifugation was carried out. After the supernatant was removed, the cells were washed thrice with PBS, and the fluorescent intensity was measured using a FACSCalibur system.

For the determination of Survivin expression, cells were harvested and washed twice in PBS. For each sample, after 100 μL fixation medium was added, the cells were incubated for 15 min at room temperature and washed once with 3 mL PBS + 0.1% NaN_3 + 5% FBS. 100 μL permeabilization medium and 10 μL CFS-conjugated anti-human Survivin or CFS-conjugated mouse IgG_1 isotype control were added and vortexed for 1–2 s. After 45 min incubation at room temperature in dark, the cells were washed once with 3 mL PBS + 0.1% NaN_3 + 5% FBS and resuspended in 500 μL PBS. The fluorescent intensity was measured using a FACSCalibur system.

2.9. Cellular uptake of DOX

MCF7 and MCF7/ADR cells were first treated with PAEN or PEIN by the same method as described in gene silencing experiment. After transfection for 48 h, the medium was replaced with fresh medium containing 2.5×10^{-3} mg/mL DOX. After 2 h incubation, the medium was replaced with fresh medium and incubation for another 2 h was carried out. Then the cells were trypsinized, washed twice with PBS and resuspended in 500 μL PBS. The fluorescent intensity was measured on a FACSCalibur system.

2.10. Cytotoxicity assay for DOX

To determine the sensitization toward DOX, MCF7 and MCF7/ADR cells were seeded at 6×10^3 cells per well in 96-well plates. After attachment, cells were treated with different PAEN or PEIN containing 1 μg RNA/well for 24 h. Then DOX solution was added at various concentrations, and MTT assay was performed after an additional 48 h. The IC_{50} value of DOX in these cells was calculated by GraphPad Prsim software.

2.11. Cell cycle assay and apoptosis analysis

Flow cytometry was used to determine the effect of PAEN treatment on cell cycle. MCF7/ADR cells were seeded in 24-well plates and incubated with different PAEN or PEIN for 24 h. Then 2.5×10^{-3} mg/mL DOX was added. After 48 h, cells were collected, washed with PBS and fixed with 70% ethanol at 4 °C overnight and treated with Rnase A for 15 min, followed by propidium iodide (PI) staining for 30 min. Cells were analyzed on a FACS Calibur.

Apoptosis was quantified by Annexin V-FITC/PI assay. MCF7/ADR cells were seeded in 24-well plates and treated with different PAEN or PEIN. After 24 h, some were incubated with 2.5×10^{-3} mg/mL DOX for 48 h. All cells were harvested and stained with Annexin V-FITC and PI following the manufacturer's instructions. Fluorescence was measured using a FACS Calibur.

2.12. In vivo RNAi experiment

Balb/c nude mice were inoculated with 100 μL of RPMI 1640 containing 1×10^7 MCF-7/ADR cells by subcutaneous injection in the left flank. At day 7 after implantation, PAPN at N/P ratio of 20 were intravenously injected at a dose of 2 mg/kg RNA. At 48 h after administration, the mice were sacrificed, and tumors were taken out and homogenized with PBS (pH 7.4). The cells were collected and the expression of P-gp and Survivin were determined.

2.13. In vivo DOX uptake

Balb/c nude mice bearing MCF7/ADR tumor were grouped and treated with PAPN containing different RNA, at a dose of 2 mg/kg RNA. At 48 h later, DOX solution (8 mg/kg) were intravenously injected. After 2 h, the mice were sacrificed, and tumors were taken out and homogenized with PBS (pH 7.4). The cells were collected and the DOX uptake was measured by FACS Calibur.

2.14. In vivo therapeutic experiment

Balb/c nude mice bearing MCF7/ADR tumor were modeling as described in Section 2.12. At day 7 after implantation, mice with visible tumors were randomly assigned to the following nine treatment groups ($n = 5$): saline control group, PAPmN group (2 mg RNA/kg), PAPsN group(2 mg RNA/kg), PAPmsN group (2 mg RNA/kg), DOX alone group (8 mg/kg), combination of aforementioned three kinds of PAPN with DOX group, and combination of PAPnN with DOX group. Mice were administered via tail vein once a week for 3 weeks, and DOX was given at 24 h after administration of PAPN. Body weight and tumor volume ([major axis] × [minor axis]^2 × 1/2, measured by calipers) of each mouse was monitored and recorded twice a week over a period of 21 days. Tumor volume on day 0 was normalized to 100% for all groups.

2.15. Statistical analyses

Student's *t*-test (two-tailed) was applied to test the significance of the difference between two groups. Differences were considered statistically significant for $^{*}p < 0.05$, and very significant for $^{**}p < 0.01$.

3. Results

3.1. Synthesis and characterization of PAP

Synthesis of PAP was successfully carried out using Michael addition reaction, which is a facile reaction between nucleophiles and activated olefins and alkynes. The amino-Michael addition to

electron-deficient carbon–carbon double bonds carries many advantages such as requiring no catalysts with mild reaction conditions, and the absence of byproducts [25]. The amine monomers were 1.5-fold molar of DSA so that the polymer was amino-ended with good water solubility. The reaction proceeded at 45 °C for 5 days to ensure an adequate degree of polymerization. The ^{1}H NMR spectra of the PAP in D_2O was in accordance with the expected structures (Fig. 1B). The methylene protons between the carbonyl of the ester bonds and the secondary amines were present at $\delta = 3.60$ ppm and $\delta = 2.54$ ppm, which were the representative signals of the newly formed compounds. The absence of signals between $\delta = 5$ and $\delta = 7$ ppm, which was assigned to the acryl group, indicated that PAP was end-capped with amino groups. The molecular weight and polydispersity of PAP measured by GPC was 10.2 kDa with Mw/Mn 2.95.

The rate of hydrolytic and reductive degradation of PAEs was presented in Fig. 1C. The degradation procedure was performed in pH 7.4 PBS at 37 °C in the absence and presence of the reduction agent DTT to simulate the physiological and reductive intracellular conditions, respectively, and monitored by GPC. PAEs degraded very slowly under physiological environment with 2%–5% decrease of Mw after 2 days and 59%–73% decrease after 20 days. However, in the present of DTT, the degradation was so rapid that the Mw decreased by 88% after 5 min.

3.2. Formation and characterization of PAEN

To be protected from ribozyme and enter the cells by endocytosis for efficient RNAi, RNA must be condensed into nanoparticles. Fig. 2A showed RNA condensation ability of PAEs at different N/P ratio from the gel retardation assay. While there was a little RNA migration at N/P ratio 1, PAEN were found to completely retard RNA migration at N/P ratios range over 5 which suggested that PAEs could form complexes completely with RNA at N/P ratios more than 5. The mean particle sizes and ζ potential as a function of N/P ratio were depicted in Fig. 2B. When the N/P ratios were 5–20, the particle sizes and ζ potential ranged in 60–110 nm and +15–30 mV, respectively. But the particle sizes of the nano-complexes at N/P ratio 1 were 170–200 nm, which were too large and perhaps resulted from the incomplete condensation of RNA. The particle sizes showed a tendency to decrease with N/P ratio increasing in contrast with ζ potential, and with the same N/P ratio, PAPN showed smaller mean particle sizes and higher ζ potential than these of PATN.

3.3. Cytotoxicity of PAEN

In MCF7/ADR cells (Fig. 2C,D), at concentration that would be used in RNAi experiments, the cell growth inhibition rate of PAEmN was lower than 6%, and still lower than 20% when the concentration was increased to 2.25-fold. The cell growth inhibition rate of PEImN was much higher than PAEmN at each concentration with 57% at highest concentration. At the concentration applied in RNAi experiments, the cell growth inhibition rate of PATsN, PAPsN and PEIsN were 17%, 25% and 14%, respectively, and increased obviously with concentrations increasing, reaching 50%, 55% and 63%, respectively, at 2.25-fold concentration, which was different from PAEmN. In MCF7 cells (Fig. 2E,F), the cytotoxicities of PAEN and PEINs were accordingly higher than that in MCF7/ADR cells, but presented a similar tendency.

3.4. In vitro shRNA expression

The iMdr-1-shRNA vector (pDNA) which contained the EGFP-encoding gene as a reporter gene was used in this work. The expression of shRNA and EGFP were coincident, i.e., the expression of EGFP could more directly reflect the tendency of shRNA expression to some extent. So the optimal N/P ratio of PAEN for RNAi could be decided by measuring the amount of EGFP. Fig. 3A and B indicated that the N/P ratios of PATN, PAPN and PEIN to reach the highest EGFP expression were 20, 20 and 10, respectively, which were chosen as the N/P ratio applied in RNAi experiments.

3.5. The influence of PAEmN on P-gp expression and DOX uptake

Comparing to that on MCF7 cells, the P-gp on the membrane of MCF7/ADR cells was markedly over-expressed (Fig. 3C), and the DOX uptake was much lower (Fig. 3D). After treated with PATmN and PAPmN, the amount of P-gp on MCF7/ADR cells was decreased to 20% and 16% of control, respectively, and the DOX uptake increased by 15 folds. In MCF7 cells, the P-gp expression and DOX uptake were hardly influenced by PAEmN.

3.6. The influence of PAEsN on the survivin expression and cell apoptosis

The Survivin expression in MCF7/ADR cells was 5.5-fold of that in MCF7 cells (Fig. 3E), and PATsN and PAPsN's treatment led to the down-regulation of Survivin protein in MCF7/ADR cells to 22% and 27% of that in control cells, respectively. In MCF7 cells, the Survivin expression also decreased by PATsN and PAPsN by 24% and 29%, respectively. The proportion of apoptosis cells induced by PATsN and PAPsN was 29% and 33% (Fig. S1), respectively. PEIsN could also induced 30% apoptotic cells, but meanwhile 9% necrotic cells.

3.7. Effect of PAEN on cytotoxicity of DOX

The cell growth inhibition rate-drug concentration curves and IC_{50} value of DOX in MCF7 and MCF7/ADR cells before and after treatment with PAEN containing various RNA were shown in Fig. 4 and Table 1. The DOX IC_{50} in MCF7/ADR cells was 33.6-fold of that in MCF7 cells, and decreased by 6.4–766.3 folds after treated with PAEN. In MCF7 cells, IC_{50} of DOX almost did not change with the addition of PAEmN and decrease by 3-fold with PAEsN treatment. PAEnN did not influence IC_{50} of DOX in MCF7/ADR cells.

3.8. The relationship between Mdr-1 and survivin genes

The effects of PAEN and PEIN containing different kinds of RNA on the P-gp and Survivin expression, DOX uptake and cell apoptosis of MCF7/ADR cells were shown in Fig. 5. A down-regulation of P-gp expression (Fig. 5A) and an increase of DOX uptake (Fig. 5C) were induced by PAEsN treatment, but to a less extent than by PAEmN. No significant variation was found on Survivin expression (Fig. 5B) and cell apoptosis in cells treated with PAEmN. PATmN and PAPmN both induced 12% apoptotic cells, while PEImN led to notable cell apoptosis (9% early phase and 9% late phase) and necrosis (7%) (Fig. S1). P-gp expression, Survivin expression and DOX uptake were all changed by PAEmsN with weaker degree than that by interfering a single gene.

3.9. Effect of combined application of PAEN and DOX on cell cycle and cell apoptosis

Fig. 6 showed that cells treated with DOX alone, PAEmN alone and DOX combined with PAEnN exhibited similar cell cycles with control cells. When MCF7/ADR cells had been incubated with PAEsN alone or DOX combining with PAEmN, PAEsN or PAEmsN, the percentage of G_0/G_1 phase and G_2/M phase were reduced, and S phase was expanded. PEIN alone or combined with DOX also changed the cell cycle, with high proportion of sub-G_1 phase.

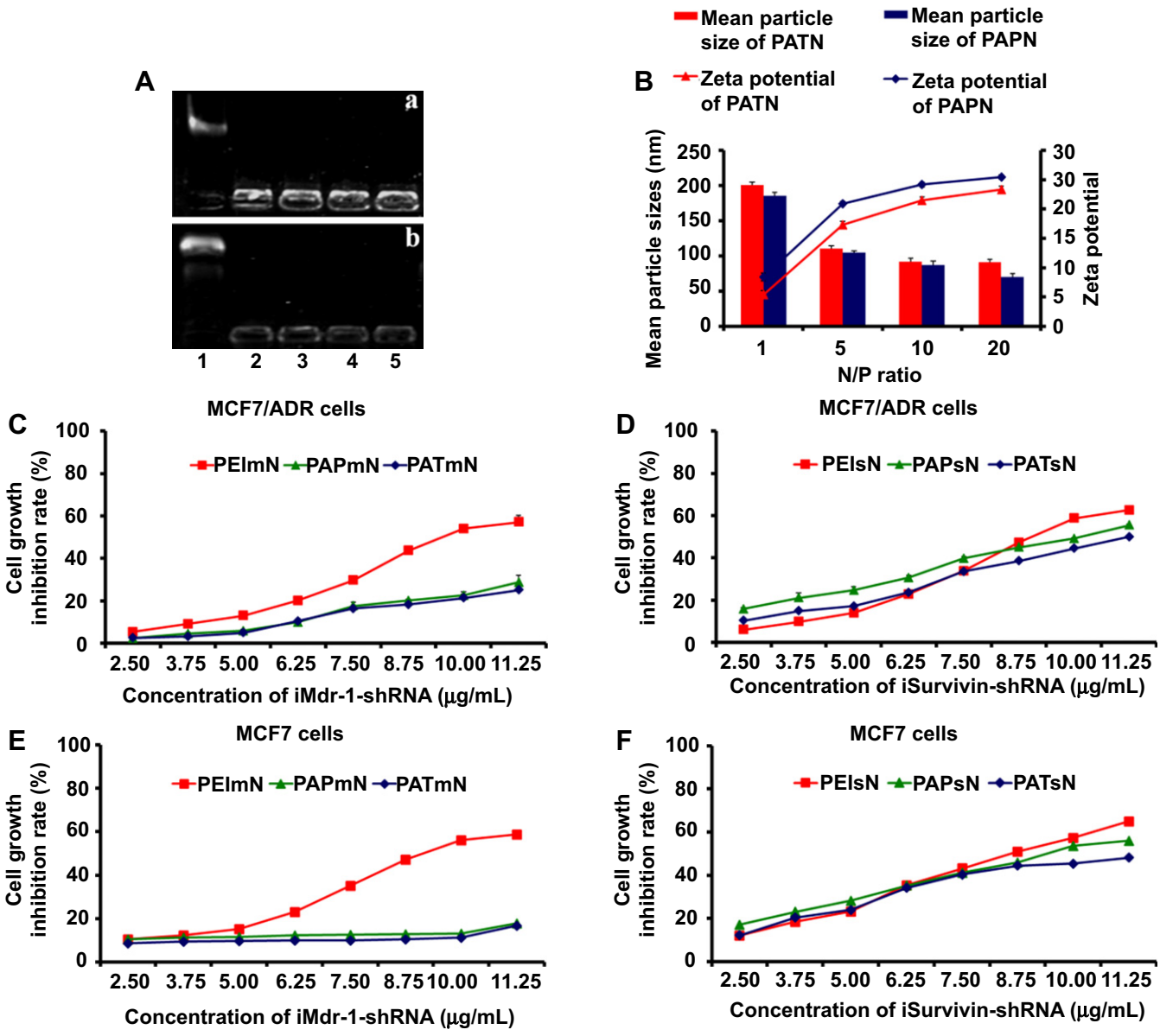

Fig. 2. Formation and characterization of PAEN. (A) Gel retardation electrophoresis of PAEs/RNA complex nanoparticles. (a) PAT, (b) PAP. Lane 1: naked RNA, Lanes 2 - 5, polyplexes prepared at N/P ratio of 1, 5, 10 and 20, respectively; (B) Mean particle sizes and ζ potential of PAEN. (C–F) Cytotoxicities of PAEN and PEIn in MCF7/ADR and MCF7 cells.

It was seen in Fig. S1 that in cells treated with DOX alone, apoptotic cells were only 8% more than control cells. When DOX was added following PAEmN, PAEsN and PAEmsN treatment, 42%–73%, 84%–85% and 86%–90% cell apoptosis were induced, respectively. Combination of PAEnN and DOX only led to 9%–13% cell apoptosis, which was similar with that caused by DOX alone, presenting clear contrast with PEInN, which induced 6% necrotic cells.

3.10. *In vivo RNAi efficiency and DOX uptake*

It was shown in Fig. 7A and B that PAPmN and PAPsN could efficiently interfere the expression of P-gp and Survivin in MCF7/ADR tumor *in vivo*, respectively. PAPmsN influenced both protein's expression, while PAPnN had effect on neither of them. DOX uptake was increased by all PAPN except for PAPnN (Fig. 7C). The results of *in vivo* experiments were consistent with those of *in vitro* experiments.

3.11. *In vivo anti-tumor effect of DOX synergized with PAEN*

When the tumor was obviously visible with about 30 mm^3, the drug resistant level of the cells extracted from tumor tissue was evaluated. Although the expressions of P-gp and Survivin were less than that in MCF7/ADR cells cultured *in vitro*, they were still much more than that in MCF7 cells, and the IC_{50} of DOX in MCF7 cells remained lower than that in *ex vivo* cells (Fig. S1). The anti-tumor efficacy of combination of DOX and PAEN was investigated in a mouse xenograft MCF7/ADR tumor model. As presented in Fig. 8, after the second administration, the tumor volumes of (PAPmsN + DOX) group and (PAPsN + DOX) group exhibited a continuously decreasing tendency, and on day 21 reached only 60% and 1.8-fold of that on day 0, respectively. The relative tumor volume of (PAPmN + DOX) group, (PAPnN + DOX) group, DOX group, PAPsN group, PAPmsN group, PAPnN gourp and saline group at day 21 was 5.2, 10.1, 11.3, 12.9, 21.5, 30.0 and 32.2, respectively. The changes of

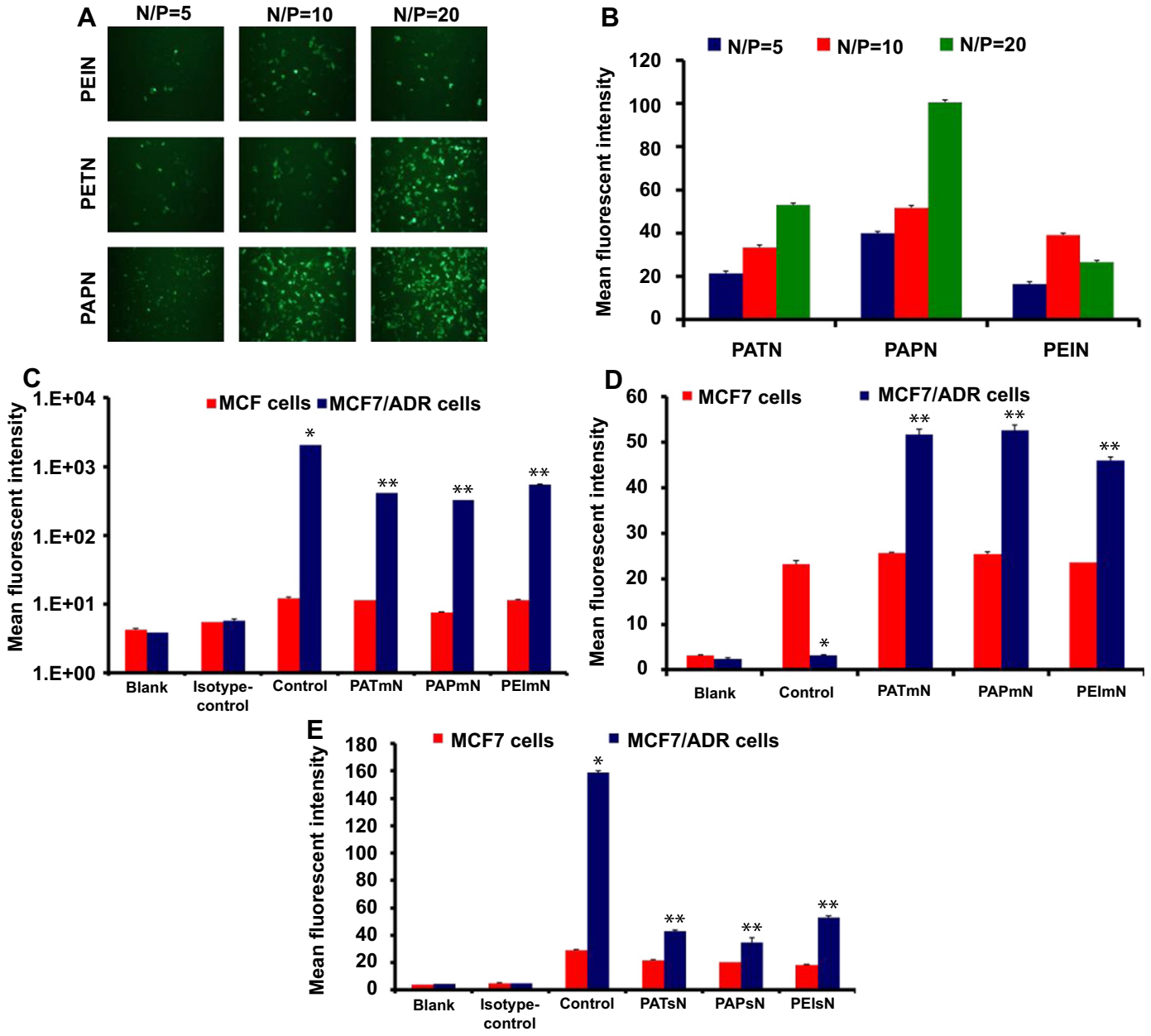

Fig. 3. *In vitro* RNAi efficiency and DOX uptake. (A) Fluorescent images and (B) quantitative measurements of GFP expression in MCF7/ADR cells transfected with PAEN and PEIN; (C) P-gp expression, (D) DOX uptake and (E) Survivin expression determined by FACS. ($^{*}p < 0.05$ compared with MCF7 cells; $^{**}p < 0.05$ compared with control group).

body weight of all groups were presented by growing curves, except for (PAPsN + DOX) group, which only showed 0.27 g loss of body weight.

4. Discussion

In our previous work, the structure-activity relationship of PAEs showed that the RNAi efficiency increased along with the increasing nitrogen atom density in the polymer backbone, and PAT showed the best RNA delivery activity in HEK 293 and U-87 MG cells [24]. However, the transfection efficiency mediated by PATN was less than 60% in MCF7/ADR cells. For promoting the RNA delivery capacity, in this work, TEPA was chosen as a new monomer to obtain higher nitrogen atom density and thus higher RNAi efficiency. The results of degradation analysis suggested that PAEs were prone to reductive destabilization in the intracellular environment, while relatively stable in physiological conditions. According to the gel retardation electrophoresis, PAEs could complete retard the migration of RNA, which suggested that the encapsulation efficiency of RNA was 100% by PAEs.

The cell growth inhibition rate, which was evaluated by MTT assays, showed that PAEmN had very low toxicity to MCF7 and MCF7/ADR cells, which exhibited superior characteristics compared with PEImN. It was worth noting that PEIsN induced less cell growth inhibition at low concentrations than PAEsN, but more cell growth inhibition at high concentrations. The reason of the cell growth inhibition caused by PAEsN and PEIsN could involve the cell apoptosis induced by reduced Survivin expression and the cell necrosis resulted from the cytotoxicity of the polymers per se. According to the cytotoxicity of PAEmN and PEImN, it could be deduced that the cytotoxicity of PAEs was very low, while PEI had much higher toxicity. So it was speculated that the primary cause of

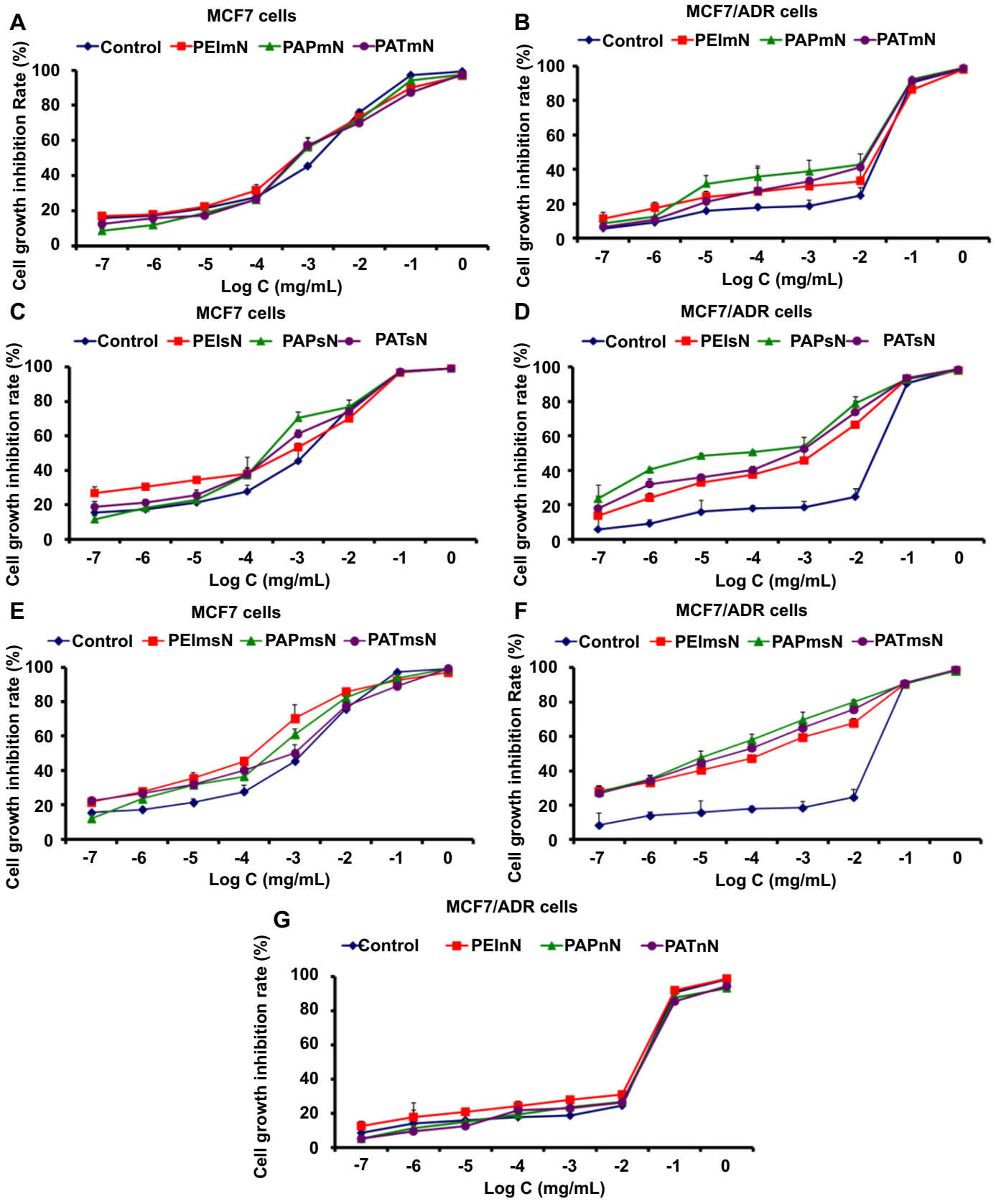

Fig. 4. DOX cytotoxicities in MCF7 and MCF7/ADR cells after treated with PAEN and PEIN. (Horizontal axis: logarithm of the concentration of DOX).

Table 1
IC_{50} of DOX in MCF7 and MCF7/ADR cells with different treatments.

MCF7 cells		MCF7/ADR cells	
Treatment	IC_{50} (mg/mL)	Treatment	IC_{50} (mg/mL)
DOX	6.303×10^{-4}	DOX	2.118×10^{-2}
PATmN + DOX	6.608×10^{-4}	PATmN + DOX	3.309×10^{-3}
PAPmN + DOX	6.389×10^{-4}	PAPmN + DOX	8.127×10^{-4}
PEImN + DOX	4.188×10^{-4}	PEImN + DOX	4.573×10^{-3}
PATsN + DOX	2.002×10^{-4}	PATsN + DOX	1.107×10^{-4}
PAPsN + DOX	1.888×10^{-4}	PAPsN + DOX	4.999×10^{-5}
PEIsN + DOX	1.258×10^{-5}	PEIsN + DOX	3.414×10^{-4}
PATmsN + DOX	1.719×10^{-4}	PATmsN + DOX	3.604×10^{-5}
PAPmsN + DOX	1.617×10^{-4}	PAPmsN + DOX	2.764×10^{-5}
PEImsN + DOX	5.500×10^{-5}	PEImsN + DOX	3.815×10^{-5}
		PATnN + DOX	1.457×10^{-2}
		PAPnN + DOX	1.395×10^{-2}
		PEInN + DOX	5.806×10^{-3}

cell growth inhibition by PAEsN was apoptosis from the down-regulation of Survivin, and PEIsN led to both apoptosis and necrosis.

The expression of P-gp of the cells was determined via the fluorescent intensity of the tag labeling the P-gp antibody. To avoid the disturbance of the fluorescence of the co-expressed EGFP, PE with red fluorescence was chosen as the tag. The P-gp expression on the membrane of MCF7/ADR cells was obviously higher than that of MCF7 cells, which might contribute to resistance of MCF7/ADR cells to DOX, a substrate of P-gp [26]. The addition of PAEmN could down-regulate the P-gp expression, i.e., PAEmN efficiently mediated the RNAi against Mdr-1 gene. But the decrease of total cellular P-gp content was not enough to prove that the MDR phenotype had been reversed, so the effect of P-gp silencing was evaluated by the cellular uptake of DOX, as the actual intracellular accumulation of DOX was more important for its efficacy. MCF7/ADR cells exhibited a significant increase of DOX uptake after treated with PAEmN, while there was almost none of DOX internalized by the cells before, indicating that the RNAi of Mdr-1 gene could enhance the DOX accumulation in MDR cells.

The expression of Survivin was also determined by FACS via the fluorescence labeling the antibody. Different from P-gp, the Survivin protein was expressed inside the cells but not on the surface of cell membranes, so fixation and permeabilization reagents were used before cells incubated with the antibody. Compared to MCF7 cells, MCF7/ADR cells showed over-expression of Survivin, which could be another one of the reasons for the drug resistance of MCF7/ADR cells. As a member of IAP family, Survivin plays a dual role in suppressing apoptosis and regulating cell division, so the cell apoptosis was supposed to be affected by the inhibition of Survivin [27]. PAEsN efficiently reduced the Survivin expression and induced cell apoptosis, indicating that PAEs also had good delivery efficiency for iSurvivin-shRNA. PEIsN exhibited comparable apoptosis-inducing ability, but with more cell necrosis, which displayed much higher cytotoxicity. The results of cell apopotosis assay verified the deduction of the cytotoxicity experiment of PAEN and PEIN.

IC_{50} value was used as criterion of the sensitivity of the cells to DOX. DOX was added following PAEN treatment, and displayed increased anti-proliferative activity in a dose dependent manner. MCF7/ADR cells exhibited strong resistance against DOX, and knockdown of Mdr-1 and Survivin did sensitize MCF7/ADR cells to DOX. PAEnN were nanoparticles complexed by PAEs and NC-shRNA, which did not target any related gene sequence. PAEnN did not influence IC_{50} of DOX in MCF7/ADR cells, which indicated that the decrease of IC_{50} value caused by PAEmN, PAEsN and PAEmsN was sequence-specific. In MCF7 cells, the P-gp expression, DOX uptake and Survivin expression were not obviously affected by PAEN, so DOX IC_{50} did not significantly decrease.

To ensure that both kinds of shRNA were condensed by PAEs completely, the amount of each shRNA in PAEmsN was half of that in PAEmN or PAEsN, and the encapsulation efficiency of RNA was

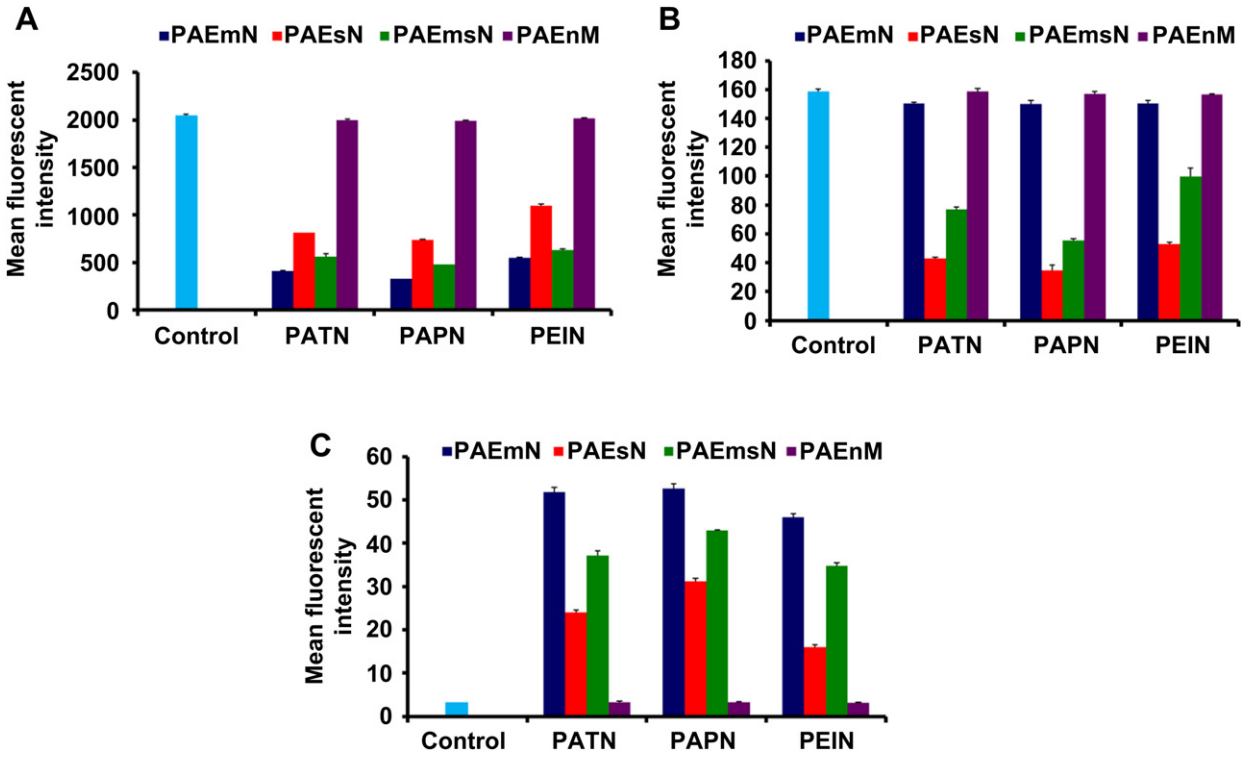

Fig. 5. Investigation of the relationship between Mdr-1 and Survivin. (A) P-gp expression, (B) Survivin expression and (C) DOX uptake in MCF/ADR cells after treated with PAEN and PEIN determined by FACS. ($^{*}p < 0.01$ compared with PAEmN, PAEsN and PAEmsN; $^{**}p < 0.05$ compared with PAEsN and PAEmsN).

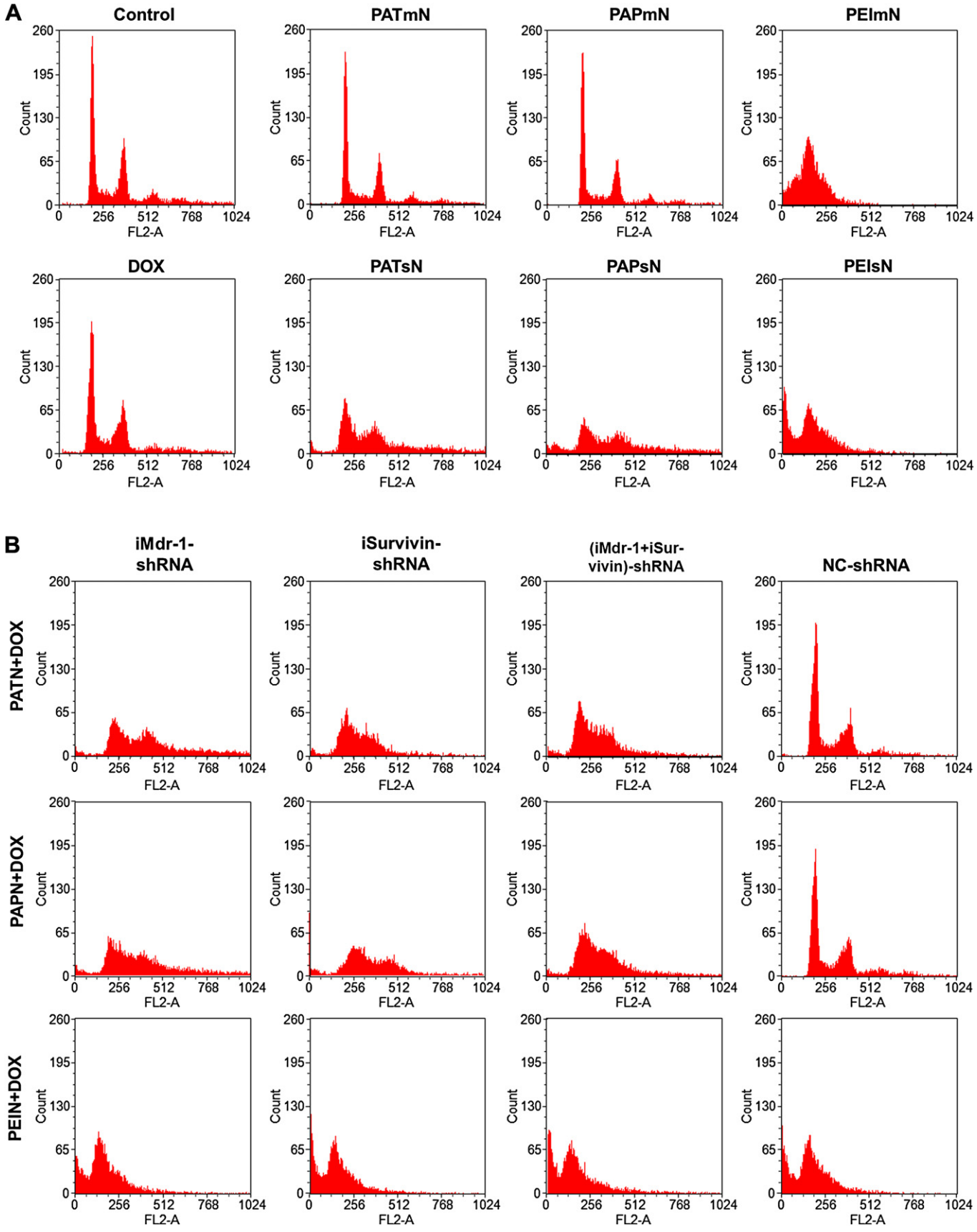

Fig. 6. Cell cycle of MCF7/ADR cells after different treatment (Including PAEN, PEIN or DOX alone and combination of DOX and PAEN or PEIN).

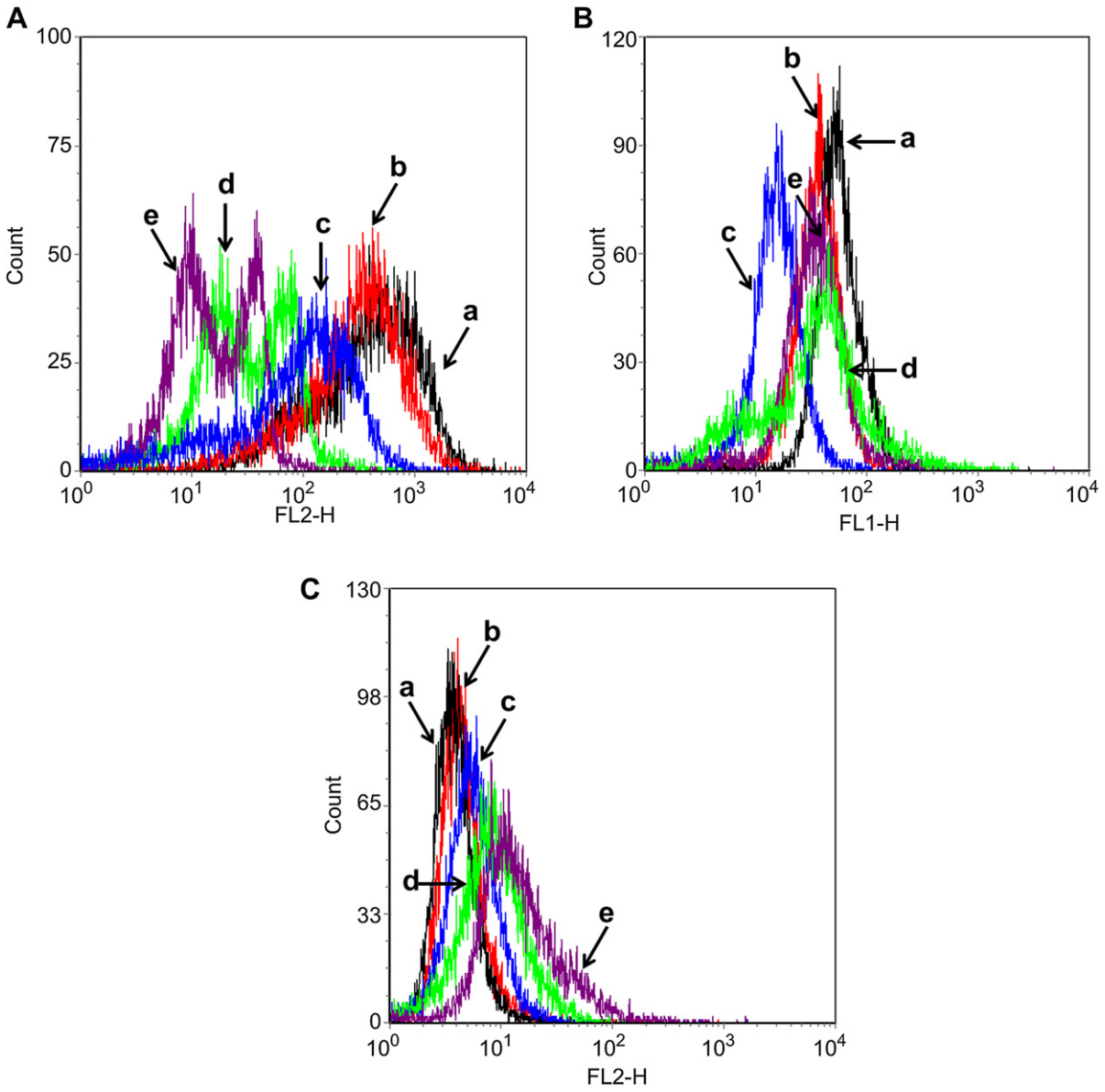

Fig. 7. *In vivo* RNAi efficiency and DOX uptake. (A) P-gp expression and (B) Survivin expression in MCF7/ADR tumor model after treated with saline (a, black), PAPnN (b, red), PAPsN (c, blue), PAPmsN (d, green) and PAPmN (e, purple); (C) DOX uptake in MCF7/ADR tumor model after treated with saline (a, black), PAPnN (b, red), PAPsN (c, blue), PAPmsN (d, green) and PAPmN (e, purple). (For interpretation of the references to colour in this figure legend, the reader is referred to the web version of this article.)

determined by gel retardation electrophoresis. It was confirmed from the gel electrophoresis assay (data not shown) that both kinds of RNA could be condensed by PAEs simultaneously, and the encapsulation efficiency of RNA reached 100%. Although the total amount of shRNA in PAEmsN equaled to that of PAEmN or PAEsN, IC_{50} value of DOX in MCF7/ADR cells treated with PAEmsN was much lower than that treated with PAEmN or PAEsN, which indicated that there was synergistic effect of the interference against two genes. In order to know the relationship of the two genes, the influence of various kinds of PAEN on corresponding protein expression, DOX uptake and cell apoptosis were evaluated. From the results, interfering Survivin affected P-gp expression, while interfering Mdr-1 did not significantly affect Survivin expression. Although PEImN could induce cell apoptosis, it might be caused by the high cytotoxicity of PEI. It was speculated that Survivin was an upstream gene to Mdr-1 and played certain role for regulating Mdr-1. Nevertheless, Survivin was not the only factor to affect Mdr-1, so PAEsN and PAEmsN had less impact than PAEmN on Mdr-1 gene. The decrease of protein expression showed consistent tendency with the concentration of RNA increasing, which illustrated that RNAi efficiency was RNA concentration-dependent in a specific range.

The genomic DNA damage caused by DOX insertion can lead to cell cycle arrest [28]. Cell cycle did not change obviously when treated with DOX or PAEmN alone, but was arrested by DOX combination with PAEmN, PAEsN or PAEmsN. It was reported that the downregulation of Survivin would retard the G1-S phase transition [29], so PAEsN alone was also able to change the cell cycle. Irreversible damage of the cells could cause apoptosis phenomena which would be tracked by the accumulation of cells in the sub G0/G1 phase [30].There was quite high proportion of sub-G_1 phase in the cell cycle of PEIN alone treated cells, which revealed the cytotoxicity of PEI from another aspect. Additionally, the generation of free radicals caused by DOX will induce cell apoptosis,

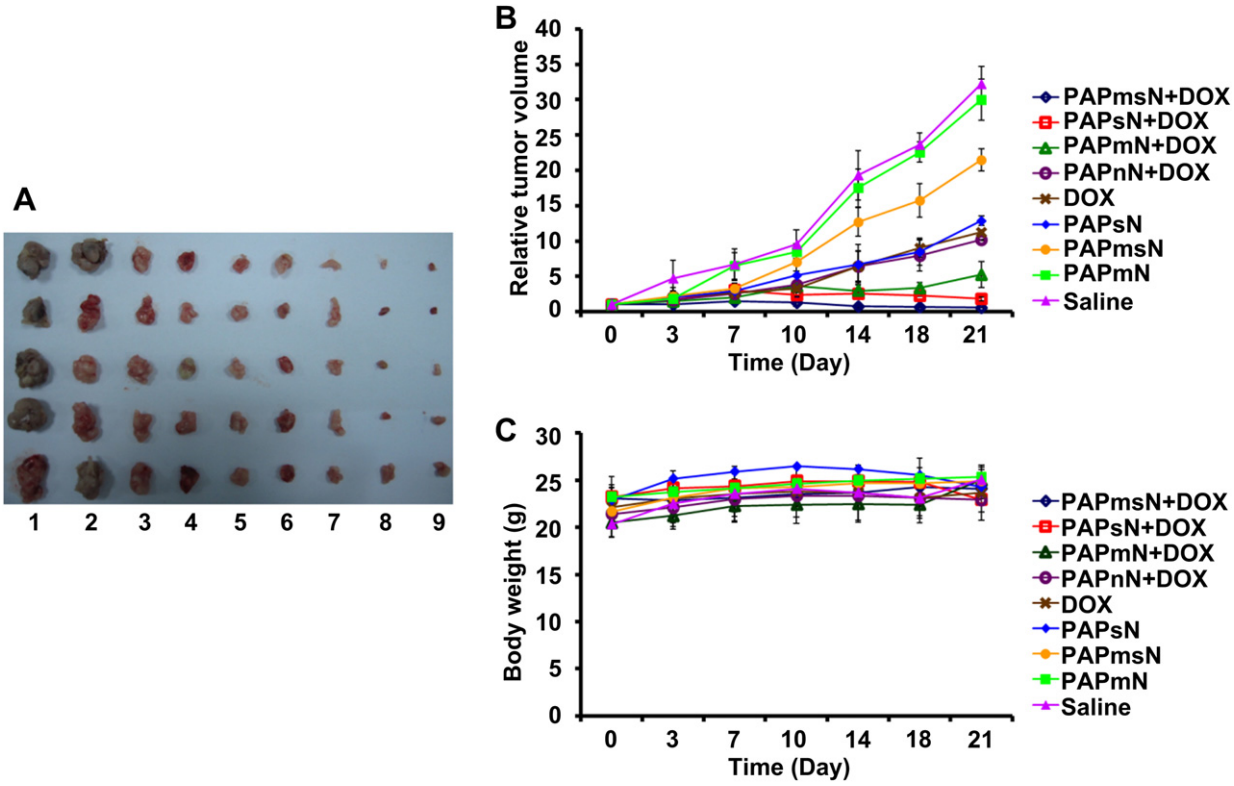

Fig. 8. *In vivo* anti-tumor effect. (A) Picture of the tumors on day 21. Line1 - 9: saline, PAPmN, PAPmsN, PAPsN, DOX, PAPnN + DOX, PAPmN + DOX, PAPsN + DOX, PAPmsN + DOX group, respectively; (B) Anti-tumor effects of PAPN, DOX or the combination of PAPN and DOX on nude mice bearing MCF7/ADR tumors; (C) Body weight of the mice bearing MCF7/ADR tumors. Data were given as mean ± SD ($n = 5$).

which is an important mechanism of DOX as an anti-tumor agent [31].The results of cell apoptosis experiment were accordant with those of cell apoptosis assay, revealing that PAEN synergized with DOX could induce MDR cells apoptosis efficiently.

The protocol of *in vivo* anti-tumor experiment was designed as following: first, treatment should begin only when the tumor reached a volume that represented a clinically relevant structure [32]; Second, it was necessary to insure that the xenograft tumor maintained the resistance against DOX; Third, the dose and frequency of PAEN and DOX administrated should not induce severe toxicity. In *ex vivo* cells extracted from the MCF7/ADR tumor, P-gp and Survivin were still over-expressed compared with MCF7 cells and the resistance to DOX was maintained in mice tumor model. According to the RNAi experiments *in vitro*, PAPN with N/P ratio of 20 introduced the highest RNAi efficiency and were chosen for *in vivo* experiments. Based on the cytotoxicity of PAEN and DOX in MCF7/ADR cells, the mice were administrated with PAPN at dose of 2 mg DNA/kg on day 1, 7 and 14, and DOX at dose of 8 mg/kg on day 1, 8 and 15, which would not induce serious toxicity. Considering that the sensitizing effect of PAPN on MDR tumor need a period for RNAi to function, DOX was administrated 24 h later than PAPN.

DOX achieved the best tumor suppression efficiency when combined with PAPmsN, which finally reduced the tumor volumes without causing body weight loss, and PAPsN and PAPmN also showed good synergy effect, which were all exceeded the therapeutic effect of DOX alone. The excellent anti-tumor effect of PAPmsN indicated that the strategy of silencing the MDR-related genes via RNAi aiming at different mechanisms of MDR had its unique advantages. Considering PAEs could condense RNA with different functions simultaneously, the anti-MDR tumor efficacy might be enhanced by introducing more RNA against other mechanisms. When combined with PAPnN, DOX did not obtain better therapeutic effect, which illustrated that the synergy effect brought by PAPN was sequence-specific. PAPsN and PAPmsN group had certain tumor inhibition effect, too, while PAPmN group did not display significant difference from saline group, which suggested that PAPmN only could enhance the anti-tumor effect of DOX but could not cause tumor suppression per se. All results above demonstrated that PAPN could efficiently promote the anti-tumor efficacy of DOX without obvious toxicity in mice bearing MDR tumor.

5. Conclusions

A new bioreducible cationic poly(β-amino esters) was designed and synthesized. The PAEs/RNA complex nanoparticles were prepared, which were efficient carriers for iMdr-1-shRNA and iSurvivin-shRNA delivery, separately or simultaneously. PAEN down-regulated the expression of P-gp and Survivin, and lowered the IC_{50} value of DOX in MDR cancer cells by 6.4–766.3 folds, via increasing intracellular DOX accumulation, arresting the cell cycle and recovering the blocked cell apoptosis pathway. In mice xenograft model bearing MCF7/ADR tumors, DOX significantly suppressed the tumor growth when combined with PAEN. Mdr-1 and Survivin are two related genes, and co-delivery of iMdr-1-shRNA and iSurvivin-shRNA had a synergistic effect on overcoming MDR. These results indicated that PAEs would be promising non-viral RNAi vectors for reversing MDR.

Acknowledgments

The National Basic Research Program of China (2010CB934000 and 2012CB932500), the National Natural Science Foundation of

China (30925041, 81102388) and Shanghai Elitist Program (11XD1406200) are gratefully acknowledged for financial support.

Appendix A. Supplementary data

Supplementary data related to this article can be found online at doi:10.1016/j.biomaterials.2012.05.039.

References

[1] Shi Z, Tiwari AK, Patel AS, Fu LW, Chen ZS. Roles of sildenafil in enhancing drug sensitivity in cancer. Cancer Res 2011;71:3735–8.
[2] Fletcher JI, Haber M, Henderson MJ, Norris MD. ABC transporter in cancer: more than just drug efflux pumps. Nat Rev Cancer 2010;10:147–56.
[3] Meads MB, Gatenby RA, Dalton WS. Environment-mediated drug resistance: a major contributor to minimal residual disease. Nat Rev Cancer 2009;9: 665–74.
[4] Giacomini KM, Huang SM, Tweedie DJ, Benet LZ, Brouwer KLR, Chu XY, et al. Membrane transporters in drug development. Nat Rev Drug Discov 2010;9: 215–36.
[5] Li YL, Duan X, Jing LH, Yang CH, Qiao RR, Gao MY. Quantum dot-antisense oligonucleotide conjugates for multifunctional gene transfection, mRNA regulation, and tracking of biological processes. Biomaterials 2011;32: 1923–31.
[6] Wang FH, Zhang DR, Zhang Q, Chen YX, Zheng DD, Hao LL, et al. Synergistic effect of folate-mediated targeting and verapamil-mediated P-gp inhibition with paclitaxel -polymer micelles to overcome multi-drug resistance. Biomaterials 2011;32:9444–56.
[7] Schmitt U, Abou El-Ela A, Guo LJ, Glavinas H, Krajcsi P, Baron JM, et al. Cyclosporine A (CsA) affects the pharmacodynamics and pharmacokinetics of the atypical antipsychotic amisulpride probably via inhibition of P-glycoprotein (P-gp). J Neural Transm 2006;113:787–801.
[8] Dönmez Y, Akhmetova L, İşeri ÖD, Kars MD, Gündüz U. Effect of MDR modulators verapamil and promethazine on gene expression levels of MDR1 and MRP1 in doxorubicin-resistant MCF-7 cells. Cancer Chemother Pharm 2011;67:823–8.
[9] Modok S, Mellor HR, Callaghan R. Modulation of multidrug resistance efflux pump activity to overcome chemoresistance in cancer. Curr Opin Pharmacol 2006;6:350–4.
[10] He QJ, Gao Y, Zhang LX, Zhang ZW, Gao F, Ji XF, et al. A pH-responsive mesoporous silica nanoparticles-based multi-drug delivery system for overcoming multi-drug resistance. Biomaterials 2011;32:7711–20.
[11] Cho HJ, Yoon HY, Koo H, Ko SH, Shim JS, Lee JH, et al. Self-assembled nanoparticles based on hyaluronic acid-ceramide (HA-CE) and Pluronic® for tumor-targeted delivery of docetaxel. Biomaterials 2011;32:7181–90.
[12] Vergara D, Bellomo C, Zhang X, Vergaro V, Tinelli A, Lorusso V, et al. Lapatinib/Paclitaxel polyelectrolyte nanocapsules for overcoming multidrug resistance in ovarian cancer. Nanomedicine; 2011. doi:10.1016/j.nano.2011.10.01.
[13] Abbasi M, Lavasanifar A, Uluda H. Recent attempts at RNAi-mediated P-glycoprotein downregulation for reversal of multidrug resistance in cancer. Med Res Rev; 2011. doi:10.1002/med.20244.
[14] Gao Y, Chen LL, Zhang ZW, Chen Y, Li YP. Reversal of multidrug resistance by reduction-sensitive linear cationic click polymer/iMDR1-pDNA complex nanoparticles. Biomaterials 2011;32:1738–47.
[15] Xiong XB, Uludag H, Lavasanifar A. Biodegradable amphiphilic poly(ethylene oxide)-block-polyesters with grafted polyamines as supramolecular nanocarriers for efficient siRNA delivery. Biomaterials 2009;30:242–53.
[16] Xue HY, Wong HL. Tailoring nanostructured solid-lipid carriers for time-controlled intracellular siRNA kinetics to sustain RNAi-mediated chemosensitization. Biomaterials 2011;32:2662–72.
[17] Wu YH, You Y, Chen ZC, Zou P. Reversal of drug resistance by silencing survivin gene expression in acute myeloid leukemia cells. Acta Biochim Pol 2008; 55:673–80.
[18] Vivas-Mejia PE, Rodriguez-Aguayo C, Han HD, Shahzad MMK, Valiyeva F, Shibayama M, et al. Silencing Survivin splice variant 2B leads to antitumor activity in taxane-resistant ovarian cancer. Clin Cancer Res 2011;17: 3716–26.
[19] Pecot CV, Calin GA, Coleman RL, Lopez-Berestein G, Sood AK. RNA interference in the clinic: challenges and future directions. Nat Rev Cancer 2011;11:59–67.
[20] Tzenga SY, Guerrero-Cázaresb H, Martineza EE, Sunshinea JC, Quiñones-Hinojosab A, Green JJ. Non-viral gene delivery nanoparticles based on poly(β-amino esters) for treatment of glioblastoma. Biomaterials 2011;32:5402–10.
[21] Ramasubramanian A, Shiigi S, Lee GK, Yang F. Non-viral delivery of inductive and suppressive genes to adipose-derived stem cells for osteogenic differentiation. Pharm Res 2011;28:1328–37.
[22] Shim MS, Kwon YJ. Dual mode polyspermine with tunable degradability for plasmid DNA and siRNA delivery. Biomaterials 2011;32:4009–20.
[23] Jere DJ, Cho CS. Biodegradable polymer-mediated sh/siRNA delivery for cancer studies. Methods Mol Biol 2010;623:243–69.
[24] Yin Q, Gao Y, Zhang ZW, Zhang PC, Li YP. Bioreducible poly (β-amino esters)/shRNA complex nanoparticles for efficient RNA delivery. J Control Release 2011;151:35–44.
[25] Fu Y, Kao WJ. In situ forming poly(ethylene glycol)-based hydrogels via thiol-maleimide Michael-type addition. J Biomed Mater Res A 2011;98:201–11.
[26] He SM, Li R, Kanwar JR, Zhou SF. Structural and functional properties of human multidrug resistance protein 1 (MRP1/ABCC1). Curr Med Chem 2011; 18:439–81.
[27] Altieri DC. Survivin, cancer networks and pathway-directed drug discovery. Nat Rev Cancer 2008;8:61–70.
[28] Bien S, Rimmbach C, Neumann H, Niessen J, Reimer E, Ritter CA, et al. Doxorubicin-induced cell death requires cathepsin B in HeLa cells. Biochem Pharmacol 2010;80:1466–77.
[29] Bian K, Fan J, Zhang X, Yang XW, Zhu HY, Wang L, et al. MicroRNA-203 leads to G1 phase cell cycle arrest in laryngeal carcinoma cells by directly targeting survivin. FEBS Lett 2012;586:804–9.
[30] Mahmoudi M, Azadmanesh K, Shokrgozar MA, Journeay WS, Laurent S. Effect of nanoparticles on the cell life cycle. Chem Rev 2011;111:3407–32.
[31] Du BY, Song W, Bai L, Shen Y, Miao SY, Wang LF. Synergistic effects of combination treatment with bortezomib and doxorubicin in human neuroblastoma cell lines. Chemotherapy 2012;58:44–51.
[32] Mena S, Rodriguez ML, Ortega A, Priego S, Obrador E, Asensi M, et al. Glutathione and Bcl-2 targeting facilitates elimination by chemoradiotherapy of human A375 melanoma xenografts overexpressing bcl-xl, bcl-2, and mcl-1. J Transl Med 2012;10:8–20.